

Wrench Analysis of Kinematically Redundant Planar CDPRs^{*}

Adhiti Raman^{1[0000-0003-0214-7586]}, Matthias Schmid^{1[0000-0002-5686-7418]},
and Venkat N. Krovi^{1[0000-0003-2539-896X]}

Clemson University, Greenville, SC 29607, USA
{adhiti.r,schmidm,vkrovi}@clemson.edu

Abstract. A fully-constrained $n - DOF$ cable-driven parallel robot (CDPR) has wrench closure if there are $n + 1$ cables exerting positive tensions spanning the wrench space. However, the quality of wrench closure is often dependent on the geometric configuration of the supporting in-parallel chains of the CDPR. The reconfigurability endowed by adding in-chain kinematic and/or actuation redundancy to a conventional cable robot could greatly improve quality of the workspace. However, the status of various joints (active, passive or locked) affect the complexity of the systematic formulation and ultimate wrench-based analysis. Past efforts have tended to equilibrate the forces in these systems in such a way as to avoid kinematic redundancies. To this end, we formulate the kinematics of the redundant reconfigurable CDPR using matrix Lie group formulation (to allow ease of formulation and subsequent generalizability). Reciprocity (and selective reciprocity) permits the development of wrench analyses including the partitioning of actuation vs structural equilibration components. The total wrench set is greatly expanded both by the addition of kinematic redundancy and selective actuation/locking of the joints. The approach adopted facilitates the holistic determination of the true wrench polytope which accounts for the wrench contributions from all actuation sources. All these aspects are examined with variants of a 4-PRPR planar cable driven parallel manipulator (with varied active/passive/locked joints).

Keywords: Wrench Analysis · Reconfigurable Cable Robot · Reciprocal Screws

1 Introduction

Traditional cable-driven parallel robots (CDPRs) are parallel manipulators whose individual chains may not feature kinematic redundancy (e.g. RPR in planar, SPS/SPU in spatial). However, due to the unilateral cable tension conditions, they require at minimum $n + 1$ cables for an $n - DOF$ task space which creates actuation redundancy.

^{*} Supported by NSF Award #IIS-1924721

2 A. Raman et al.

The placement of the cable winching mechanism on a mobile platform allows the ability to change the geometry of the attachment points of the cables creating a reconfigurable CDPR (r-CDPR). Such additional kinematic and/or actuation redundancy creates potential for enhancing the performance of conventional cable robots. For example, the added mobility offers advantages such as the ability to increase the wrench feasible workspace (WFW) as proposed by Rosati et al. [20] or improve the quality of the WFW for a span of end-effector poses. This mobility can be incorporated by housing the winching mechanism on mobile differential drive robots that are independently steered, as seen in [17], or looping the cable through a pulley on linear guides as modeled and implemented in [24]. While early efforts [4] speculated on the value of adding reconfigurability to CDPRs, specifically the location of the control and actuator packages, this prospect was not fully analyzed until later. Zhou [23] used the reconfigurability offered by an r-CDPR with mobile attachment points to adjust cable tensions to suit the task and modulate control the stiffness at the end-effector. Nyugen et al. [16] proposed an r-CDPR alternative to maintenance lifts in aircraft hangers and resolved the redundancy by optimizing for stiffness and power consumption. Rasheed et al. [19] proposed a spatial r-CDPR wherein the columns supporting the fully-constrained CDPR are independently movable on differential drive robots (forerunner to [17]). Gagliardini et al. [11] presented a spatial reconfigurable cable robot for sandblasting and painting of large structures and proposed an optimization algorithm for planning the reconfiguration. Erskine et al. [8] performed the wrench analysis on a reconfigurable robot where the cable lengths are kept constant and the cable attachment points are connected to drones. In our own past work, we have used base mobility in combination with the tension isolation module developed by Zhou [23] on a 3-cable planar r-CDPR to modulate the stiffness at the end-effector [18].

The modeling and formulation for CDPRs have largely relied on vector loop closure. In some papers, this relationship has also been easily derived through screw theoretic analysis as described in Bosscher et al. [2]. For a fully-constrained CDPR, the force and moment applied on the payload is related to the cable tension directly by J^T (which is composed of the wrenches along the cables). Traditionally, cables have been modeled as unilateral prismatic joints surrounded by two passive revolute joints, i.e. they can exert forces along an axis, in a certain direction. Such a formulation treats the cable and attachment points as a "proper" serial chain (3 joints for 3 degrees of freedom at the end-effector). In effect the cable is treated as a two force member (in the planar case) and defines the direction of the line of action of a pure force. If the attachment points of the cables are known, one can write down the equations of static equilibrium in a matrix form where the columns of the subsequent Jacobian form the pure force direction and the magnitudes of the forces are unknown. Such a formulation makes it amenable for subsequent linear matrix analysis. Although this has proven adequate for CDPRs, the formulation and wrench analyses r-CDPRs has not yet been undertaken without decoupling the mobile base attachment points from the CDPR. In this paper we systematically formulate and analyze a planar

r-CDPRs with multiple cases of in-chain kinematic and actuation redundancy by varying status of joints (active/passive/locked). We formulate the kinematics using reciprocal screw theory [1] applied using matrix Lie group formulation following the formulation style and notation in Murray et al. [15]. The use of reciprocity, selective reciprocity with matrix Lie groups permits the systematic, analytical and computationally-efficient treatment of r-CDPRs as a sub-class of articulated multi-body systems as well as ease of generalization to the fully-spatial case.

Further, while there have been many studies encompassing wrench feasibility analyses of CDPRs [3, 12, 13, 5], these do not consider the effect of kinematically-redundant supporting chains. Even in the studies by Erskine [8] and Rasheed [19] that deal specifically with the wrench analysis of reconfigurable CDPRs, the forces at the payload and mobile bases are equilibrated separately. Therefore, the determined wrench set available at the end-effector does not directly take into consideration the wrench contributions at the mobile joints. The separation of the force equilibration also necessitates the redundancy resolutions to take cascaded forms where the actuation and kinematic redundancies are resolved asynchronously. In contrast, we have reformulated the kinetostatics to consider these forces within the same wrench Jacobian and also determine the true wrench set available at the end-effector.

The wrench set determination was carried out with the convex hull method described by Bouchard [5]. Studies by Bosscher [3], Firmani [9, 10] and Boudreau [6] all consider the convex hull determination for examining the available wrench set for parallel structures. Boudreau specifically tackles the problem of a kinematically redundant (rigid-link) planar parallel manipulator and shows that the convex hull, sliced at $m_z = 0$ for all possible kinematic configurations of the redundant manipulator presents the same results as the optimization schema to produce maximum forces at the end-effector for a kinematically redundant 3-RPRP manipulator by Weihmann [21].

In this work, after a brief introduction of the mathematical background (in Section 2), we represent the formulation of the r-CDPR using Lie groups (in Section 3.1) by following the procedure and notation established in [15]. In subsequent sections of this paper we model the reciprocal wrenches that span the wrench space of the r-CDPR (Section 3.2) and discuss how the in-chain redundancies improve the dexterity and wrench set of the manipulator. Finally, a study of wrench feasibility shows the value added by the redundancy and is demonstrated in the paper with the analysis and visualization of available wrench sets (and how they change shape) at the end-effector through graphical representations of its wrench polytope (Section 4).

2 Mathematical Methods

2.1 Lie Group Formulations

Lie groups are a group of symmetry transformations that form smooth differentiable manifolds. Lie groups include rotations, translations, scaling, and

4 A. Raman et al.

other geometric transformations. Despite the many parallels existing between the unilateral tension requirements and unidirectional normal-force constraints arising in multi-fingered hands, multi-legged walkers and multi-arm cooperative-manipulation, efforts to relate this wealth of literature to cable robots have been very limited. Such an approach offers us an opportunity to pursue a coordinate-free geometric formulation as well as connect this formulation to the rich literature of geometric treatment of articulated in-parallel multibody systems.

The notation for the Lie group formulation is largely based on the notation in [15], where $\{s\}$ forms the inertially-fixed spatial frame and $\{b\}$ forms the body-fixed or moving frame and homogeneous transformation of the body-fixed frame with respect to the spatial frame is given by $g_{sb} \in SE(3)$. In vector space, the body twist is ${}^b t_{sb} = [v \ \omega]^T$ and is related to the spatial twist by an adjoint transformation, ${}^s t_{sb} = Ad_{g_{sb}} {}^b t_{sb}$ where $Ad_{g_{sb}} = \begin{bmatrix} R_{sb} & \hat{p}_{sb} R_{sb} \\ 0 & R_{sb} \end{bmatrix}$ (in planar:

$$Ad_{g_{sb}} = \begin{bmatrix} R_{sb} & \begin{bmatrix} p_y \\ -p_x \end{bmatrix} \\ 0 & 1 \end{bmatrix}).$$

2.2 Reciprocal Wrenches

There have been many successful attempts to unify the terminology and formulation surrounding the design of parallel robots. In [7], Bruyninckx proposes a unified method of wrench formulation using screws that is equally applicable to the formulation of serial-chain as well as in-parallel manipulators.

For a given serial chain, each column of its Jacobian, J , represents the partial twist at the end-effector which is contributed by that joint. In other words, it is the instantaneous motion of the end-effector caused by the i th joint when all but the i th joint is locked [14]. The span of the all the twists that make up a Jacobian is called the twist space of the robot.

A *reciprocal wrench* is then any wrench that is reciprocal to a twist in the span of J such that, $w_r^T t = 0, \forall t \in span(J)$. In other words, given a serial chain the reciprocal wrench to the twists that form the Jacobian will be that set of wrenches that does zero work on $t \in span(J)$. The wrench will then belong to the null space of the Jacobian. The number of reciprocal wrenches that exist will be $(6 - n)$ for spatial and $(3 - n)$ for planar, where $n = rank(J)$.

A *selectively non-reciprocal wrench* (SNRW) is a special case of reciprocal wrenches. It is a wrench that is reciprocal only to the i^{th} twist and non-reciprocal to all other joints.

$$w_r^T t = \delta_i \text{ with } \begin{cases} (\delta_i)_j = 1, & \text{if } i = j \\ (\delta_i)_j = 0, & \text{if } i \neq j \end{cases} \quad (1)$$

The SNRW of a joint is the partial wrench at the end-effector contributed by joint i . In this sense it is analogous to the assembly of partial twists forming the twist Jacobian. The assembly of the SNRW for each of the joints forms the

wrench Jacobian, J_w . For some unique cases, (e.g. a serial robot) this Jacobian is the same as the transpose of the twist Jacobian, J . The selectively non-reciprocal wrench (or screw) described here is the same as the special case of reciprocal screws described by Agrawal [1].

2.3 Available Wrench Set

The Available Wrench Set (AWS) is the set of all forces at the end-effector that are achievable without violating the force limits at the actuated joints. These limits are determined by the setting the joint torques to their extreme values and plotting the limits of wrenches they cause at the end-effector. Bouchard et al. [5] determined that the zonotope generated at the end-effector for an equilibrated system is a convex polytope called the wrench polytope. The wrench limits can also be determined as ellipsoids, tangential to the manipulability ellipsoids introduced by Yoshikawa [22]. However, as the ellipsoids an approximation of the wrench polytope, they do not represent the AWS in its entirety and thus not considered here.

2.4 Wrench Polytope

The wrench polytope is a region of end-effector wrenches determined by the bounds on the range space of joint forces. For the planar case, this polytope is graphically represented by a three dimensional shape in the task space. Given the current pose of the end-effector, the vertices of the polytope are determined by mapping the extreme values of the joint torques ($f_i \in \{f_{max}, f_{min}\}$) to task space wrenches using the wrench Jacobian. If the number of actuated joints in a parallel robot is given by n , then the resultant number of vertices forming the polytope is given by 2^n ,

$$F_{o_{ext}} = J_w f_{c_{ext}}; f_{c_{ext}} = [f_{1_{ext}} \quad f_{2_{ext}} \quad \dots \quad f_{n_{ext}}]^T$$

where n is the number of actuators and $f_{n_{ext}}$ represents an extreme value of f_i .

For the redundant manipulator, a number of these vertices thus determined lie inside the overall convex hull. However, the internal facets determined by connecting all the (internal and external) vertex points also represent $n - 2$ actuators working at the extreme limits.

3 r-CDPR Formulation

All these aspects are examined with variants of a 4-PRPR planar cable-driven parallel manipulator (with varied active/passive/locked joints) to serve as an exemplar of the reconfigurable CDPRs (r-CDPR) under study. In the rest of the paper, we will use the following notation for the planar 4-PRPR with frames as shown in Figure 1.

We define the payload or end-effector as a rigid body connected via cables to the main frame or to sliders that move along the main frame. The cables

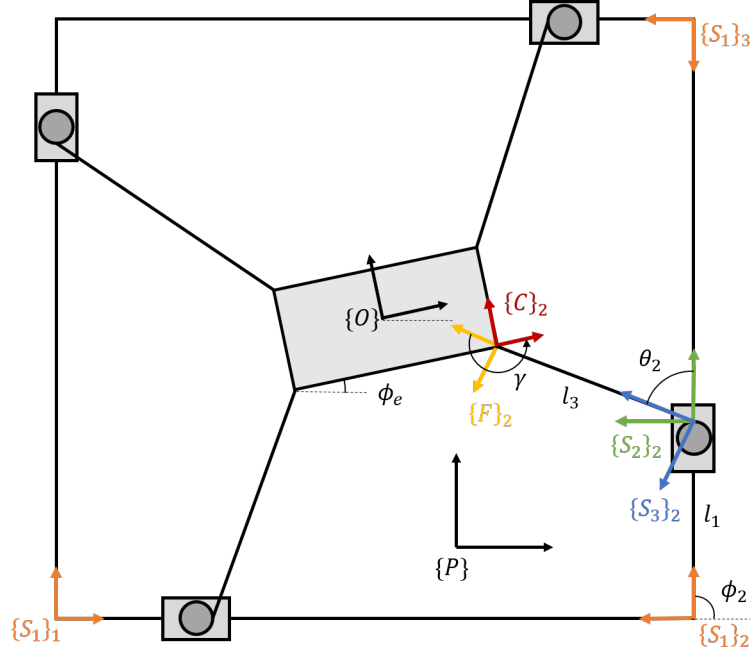


Fig. 1. Planar 4-PRPR CDPR (Planar r-CDPR)

are considered to have no mass and no slack, and the sliders moving along the frame are not inhibited by friction. The world frame and end-effector frame are denoted by $\{P\}$ and $\{O\}$ respectively. The frame corresponding to the geometry of the CDPR are given by $\{S_1\}_i$ where i corresponds to the i^{th} chain. Every subsequent frame in the chain is given by $\{S_j\}_i$ for j joints in each chain. The final frame in the chain, the frame that shares an origin with the contact point on the surface, is given by $\{F\}_i$. The contact point of each cable with the end-effector is given by $\{C\}_i$, and it is assumed that the orientation of $\{C\}_i$ is fixed with respect to $\{O\}$. The angle between $\{F\}_i$ and $\{C\}_i$ is γ_i .

3.1 Twist Assembled Jacobian

For the i^{th} serial chain, the twist from its base frame $\{S_1\}_i$ to final frame $\{F\}_i$ is given by $t_{s_1 f}^{s_1}$. Dropping subscript i ,

$$t_{s_1 f}^{s_1} = [t_{s_1 s_2}^{s_1} \quad t_{s_2 s_3}^{s_1} \quad \dots \quad t_{s_n f}^{s_1}]$$

$$t_{s_1 f}^{s_1} = [\hat{t}_{s_1 s_2}^{s_1} \quad Ad_{g_{s_1 s_2}} \hat{t}_{s_2 s_3}^{s_2} \quad \dots \quad Ad_{g_{s_1 s_n}} \hat{t}_{s_n f}^{s_n}] \begin{bmatrix} \dot{q}_{01} \\ \dot{q}_{12} \\ \vdots \\ \dot{q}_{n-1,n} \end{bmatrix}$$

$$t_{s_1 f}^{s_1} = J_{s_1 f}^{s_1}(q) \dot{q}_i = J_s(q) \dot{q}_i$$

Each column of the twist assembled Jacobian or the structure Jacobian, $J_s(q)_i$, forms the twist between two consecutive frames, $k-1$ and k , expressed in the spatial frame $\{S_1\}$ by adjoint transformations, ${}^F t_{k-1,k} = Ad_{g_{F,k-1}}^{k-1} t_{k-1,k}$.

The attachment point of a cable on the payload the the cable robot is analogous to a the modelling of a finger contact on a grasped object by Murray, Li and Sastry [15]. The wrench contribution from tension in the cable is along the direction of $\{F\}_i$ applied on $\{C_i\}$. This wrench is given by F_{c_i} ,

$$F_{c_i} = \begin{bmatrix} -\cos(\gamma) \\ -\sin(\gamma) \\ 0 \end{bmatrix} f_i, \forall f_i \geq 0$$

where f_i is the magnitude of the tension. Transforming this force into the object frame $\{O\}$,

$$F_{O_i} = Ad_{g_{oc_i}}^T F_{c_i} = Ad_{g_{oc_i}}^T N_{c_i} f_i = P_i f_i$$

where N_{c_i} is the direction vector of the i^{th} cable with respect to the contact frame $\{C_i\}$, and P_i is the i^{th} column of the pulling map. The total wrench is the summation of the individual i^{th} contributions. As the contact point is fixed to the object, the relative velocity between the contact frame and the cable frame is zero in x, y and z . Thus the relationship $N_{c_i}^T t_{f_i c_i}^{c_i}$ equals zero. With this relationship follows the computation of the relationship between the active and passive joint twists of serial chain and twist at the end-effector. The complete derivation is given in [15] for the analogous case of multi-fingered grasping.

The forward-kinematic relationship (joint- to task-space) for the manipulator is given by,

$$J_c = \begin{bmatrix} N_{c_1}^T Ad_{g_{s_1 c_1}}^{-1} J_{s_1 f_1}^{s_1}(q_{f_1}) & & 0 \\ & \ddots & \\ 0 & & N_{c_k}^T Ad_{g_{s_k c_k}}^{-1} J_{s_k f_k}^{s_k}(q_{f_k}) \end{bmatrix}$$

$$J_c \dot{q} = P^T t_{p_o}^o$$

where P is the pulling map and J_c is the cable Jacobian, analogous to the grasp map and hand Jacobian. For the fixed base standard case, the cable Jacobian is an identity matrix.

3.2 Wrench Assembly

The body twist at $\{O\}$ for a single chain is given by,

$$t_{s_1 o}^o = Ad_{g_{s_1 o}}^{-1} J_{s_1 o}^{s_1}(q) \dot{q}_i$$

8 A. Raman et al.

For the 4-cable planar r-CDPR, this is

$$\begin{bmatrix} \dot{x} \\ \dot{y} \\ \dot{\phi} \end{bmatrix} = \begin{bmatrix} \cos(\gamma + \theta_2) & y_{oc} + l_3 \sin \gamma & \cos \gamma & y_{oc} \\ -\sin(\gamma + \theta_2) & l_3 \cos \gamma - x_{oc} & -\sin \gamma & -x_{oc} \\ 0 & 1 & 0 & 1 \end{bmatrix} \begin{bmatrix} \dot{l}_1 \\ \dot{\theta}_2 \\ \dot{l}_3 \\ \dot{\gamma} \end{bmatrix}$$

where l_1 and l_3 are the linear translations, which can be locked, passive or active and θ_2 and γ are the passive rotations.

Case 1: Passive motion accommodation (4-PRPR) If the entire system is passive, the system should be able to accommodate any arbitrary twist applied at the end-effector. The total rank of the assembled Jacobian for a singular chain is 3, while the dimensions of its columns is four. Thus, there is a linear dependency that must exist between the columns. However, we see that at any time, at least 3 of the four columns are independent and is thus able to passively accommodate any twist at the end-effector except when $l_3 = 0$ or when $\theta_2 = 0$. For these conditions, another set of columns becomes linearly dependent thus reducing the rank to 2.

Case 2: Standard, fully-constrained CDPR (4-RPR): With the mobile bases locked and fixed, each individual chain forms a planar RPR serial chain attached at the end-effector and twists associated with the locked joint drop out of consideration. Thus each chain forms a class-1 type ‘‘proper’’ serial chain, where the *DOFs* of the joint equal the *DOFs* at the end-effector. The wrench at the end-effector is contributed to only by the actuated joint. The SNRW at this joint is given by,

$$[t_{\theta_2} \ t_{\gamma}]^T w_{l_3} = 0$$

$$w_{l_3} = \begin{bmatrix} -\cos \gamma \\ \sin \gamma \\ x_{oc} \sin \gamma + y_{oc} \cos \gamma \end{bmatrix}$$

Assembling the wrenches for all the four chains, we get,

$$[w_{l_{3_1}} \ w_{l_{3_2}} \ w_{l_{3_3}} \ w_{l_{3_4}}] \begin{bmatrix} f_{c_1} \\ f_{c_2} \\ f_{c_3} \\ f_{c_4} \end{bmatrix} = F_o$$

The assembled wrenches form the wrench Jacobian \mathbf{J}_w which takes the same form as the pulling map, \mathbf{P} .

Case 3: Reconfigurable CDPR (4-PRPR) Each chain connecting to payload is a 4-*DOF* PRPR mechanism. Thus, each chain forms a class-3 type redundant serial chain. Any wrench at the end-effector will have a non-unique and possibly undefinable contribution at the joint. Thus, we break each chain off after the first 3 (PR) joints to form a “proper” serial chain. Any wrench at frame $\{F\}$ will have a unique solution at the joints. The forces on the payload from these wrenches are then summed and translated into the body frame at $\{O\}$.

$$[t_{\theta_2} \ t_{l_3}]^T w_{l_1} = 0$$

$$[t_{\theta_2} \ t_{l_1}]^T w_{l_3} = 0$$

$$w_{l_1}^f = \begin{bmatrix} 0 \\ -1 \\ l_3 \end{bmatrix}$$

$$w_{l_3}^f = \begin{bmatrix} -\sin(\theta_2) \\ -\cos(\theta_2) \\ l_3 \cos(\theta_2) \end{bmatrix}$$

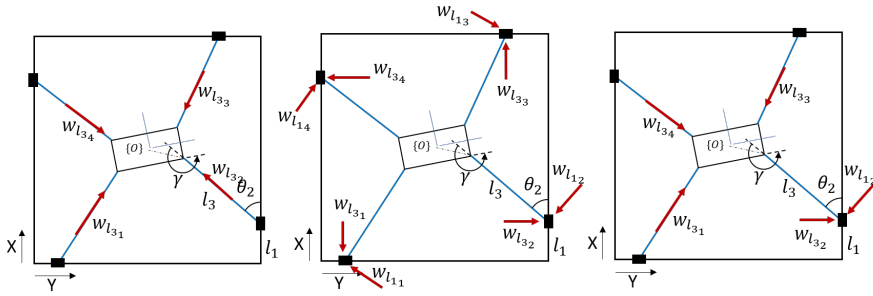


Fig. 2. Lines of action of reciprocal wrenches on a 3-*DOF* planar model for (a) Case 2, (b) Case 3 and (c) Case 4

These wrenches are then transformed to the body-frame $\{O\}$.

$$w_{l_1} = Ad_{g_{of}}^T w_{l_1}^f = \begin{bmatrix} -\sin(\gamma) \\ -\cos(\gamma) \\ l_3 - x_{oc} \cos(\gamma) + y_{oc} \sin(\gamma) \end{bmatrix}$$

$$w_{l_3} = Ad_{g_{of}}^T w_{l_3}^f = \begin{bmatrix} -\sin(\gamma + \theta_2) \\ -\cos(\gamma + \theta_2) \\ l_3 \cos(\theta_2) - x_{oc} \cos(\gamma + \theta_2) + y_{oc} \sin(\gamma + \theta_2) \end{bmatrix}$$

10 A. Raman et al.

The collected wrench Jacobian is an assembly of individual wrenches. The lines of actions of these forces are given in Figure 2. For a CDPR, the direction of the forces should be such that they always provide positive tensions at the cables.

Case 4: Single mobile base (3-RPR, 1-PRPR): We break each chain at the point connecting to the payload $\{C_i\}$ and the forces at $\{C_i\}$ are translated into the $\{O\}$ frame. The 3 RPR chains form a 2-DOFRP “deficient” serial chain. Any wrench at frame $\{F\}$ will have non-unique solutions at the joints. Given a reciprocal wrench for the entire chain, the SNRWs will be the set of reciprocal wrench minus the wrench reciprocal to the entire chain. The forces on the payload from these wrenches are then summed and translated into the body frame. The reciprocal wrench for the entire chain given by,

$$[t_{\theta_2} \ t_{l_3}]^T w_r = 0; w_r = \begin{bmatrix} 0 \\ -1 \\ l_3 \end{bmatrix}$$

For each joint there exist two wrenches spanned by the null space. For the active joint these are,

$$W_{l_3} = \begin{bmatrix} 1 & 0 \\ 0 & -1 \\ 0 & l_3 \end{bmatrix}$$

As one of these screws corresponds to the reciprocal wrench for the entire chain, it cannot be unique, and thus the true selective reciprocal wrench is given by the first column. The SNRWs for the remaining chain are described in Case 3. The wrenches are transformed from frame $\{F\}$ to frame $\{O\}$ as before and we see that the wrench contribution of the individual cables takes a form similar to Case 2, as expected.

$$W_{O_i} = \begin{bmatrix} -\cos(\gamma) \\ \sin(\gamma) \\ x_{oc} \sin(\gamma) + y_{oc} \cos(\gamma) \end{bmatrix}$$

Assembling the wrenches, we extract a wrench Jacobian of size 3 by 5 where 5 is the number of actuated joints.

4 Analysis of the Available Wrench Set

The following section contains a study on the determination of the wrench set available at the end-effector for two of the cases described above. This is done by investigating the convex polytopes generated by joint actuators at their extreme values. Any wrench at the end-effector that can be sustained by the joints must lie within the boundaries of that polytope.

The wrench-feasible workspace (WFW) of a parallel cable-driven mechanism is the set of poses of its mobile platform for which the cables can balance any wrench in a specified set of wrenches, such that the tension in each cable (as well as the forces at the mobile bases for an r-CDPR) remains within a prescribed range. The boundaries of the WFW are determined by the geometric properties of the Available Wrench Set [3].

Traditionally, the AWS is determined only by the tension contribution of the cables. Even in studies of reconfigurable robots, the wrench contributions of the mobile bases are analysed independently. In this paper, we will make use of the formulations in Section 3 to visualize the combined wrench set.

We assume that the cables contain negligible mass and have no slack even at minimum tensions. The end-effector is a rigid body and the dynamic effect of gravity is considered negligible as well. The frame of the planar manipulator is $1 \text{ m} \times 1 \text{ m}$, and the platform is $0.39 \text{ m} \times 0.16 \text{ m}$. The minimum and maximum forces at the cables ranges from 0 N to 1 N and at the mobile base prismatic joints from -0.1 N to 0.1 N .

The quality of the Available Wrench Set provides an indication of the quality of the wrench feasible workspace at that point, but does not give an indication of the overall quality of the workspace over a span of poses. Future efforts will involve determining the quality of the wrench feasible workspace around the locii of the current pose to update the limits of the available end-effector wrenches and twists for input into r-CDPR control.

4.1 Available Wrench Set for the 4-RPR CDPR

The wrench polytope of the 4-RPR CDPR is shown in Figure 3. As expected, the number of vertices for the wrench polytope are 16, as there are 16 combinations of maximum torques at the end-effector. The red hypercube in Figure 3 encapsulates the set of wrenches for which the magnitude of tension in cable 1 is maximum and the green hypercube encapsulates the set of wrenches for which the magnitude of the tension in cable 1 is at its minimum. The regions between them and within the polytope shows the region in which this actuator works under its torque capabilities, but another set of actuators sustains extreme values. The polytope generated at $\phi = 0$ is symmetric along all three axis. It contains 14 external vertices and two internal vertices with are coincident. This marks points where all of the actuators have either their maximum or minimum values. This is aligned with intuition. To achieve zero wrench at the end-effector all of the forces at the joints should either be fighting against each other or be zero. The closer the pose moves towards the extreme value of orientation ($\phi = -0.4$ or 0.4), the less it is able to sustain a moment in that same direction. This is seen by the polytope moving further along the positive m_z axis as the pose moves to $\phi = -0.35$ and along the negative axis when the pose moves to $\phi = 0.35$. At these positions, the cable actuators are less able to sustain transition actuator values, as seen by either disappearing hypercubes for cable 1 in Figure 3 (b) or fully aligned hypercubes in Figure 3(c). The polytopes become truly cuboidal at

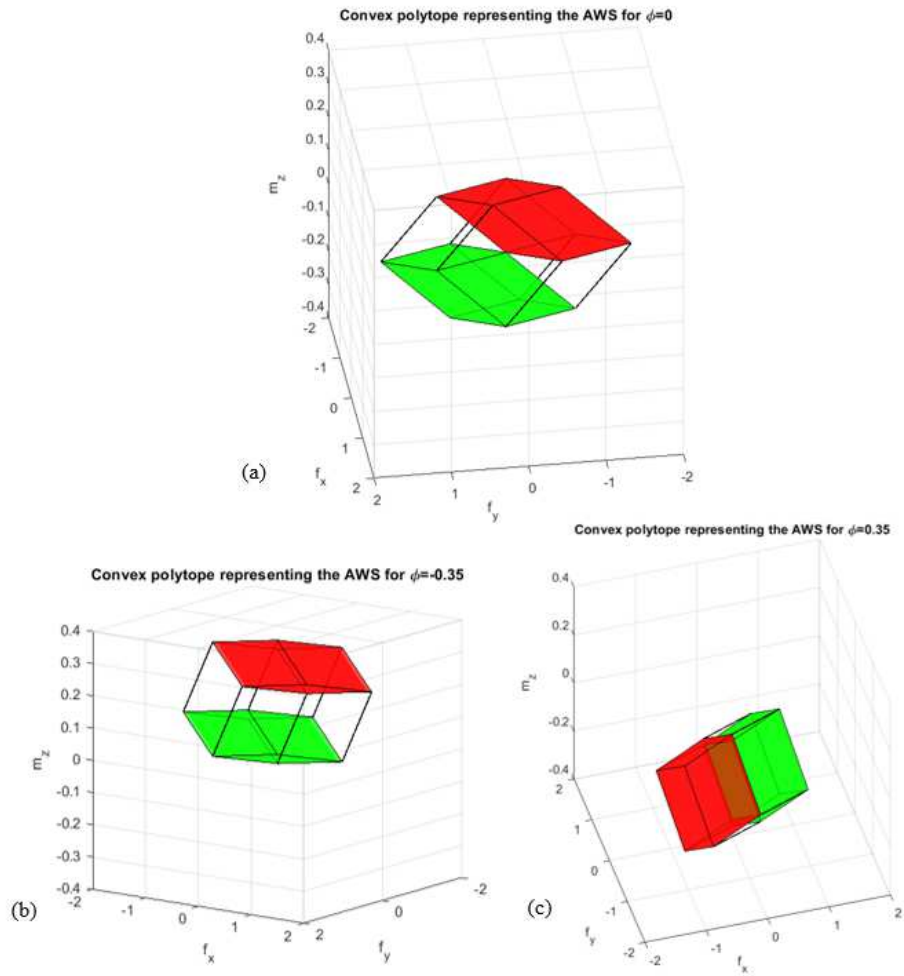


Fig. 3. Convex polytope representing AWS for the 4-RPR CDPR at (a) $\phi_e = 0$ (b) $\phi_e = -0.35$ and (c) $\phi_e = 0.35$

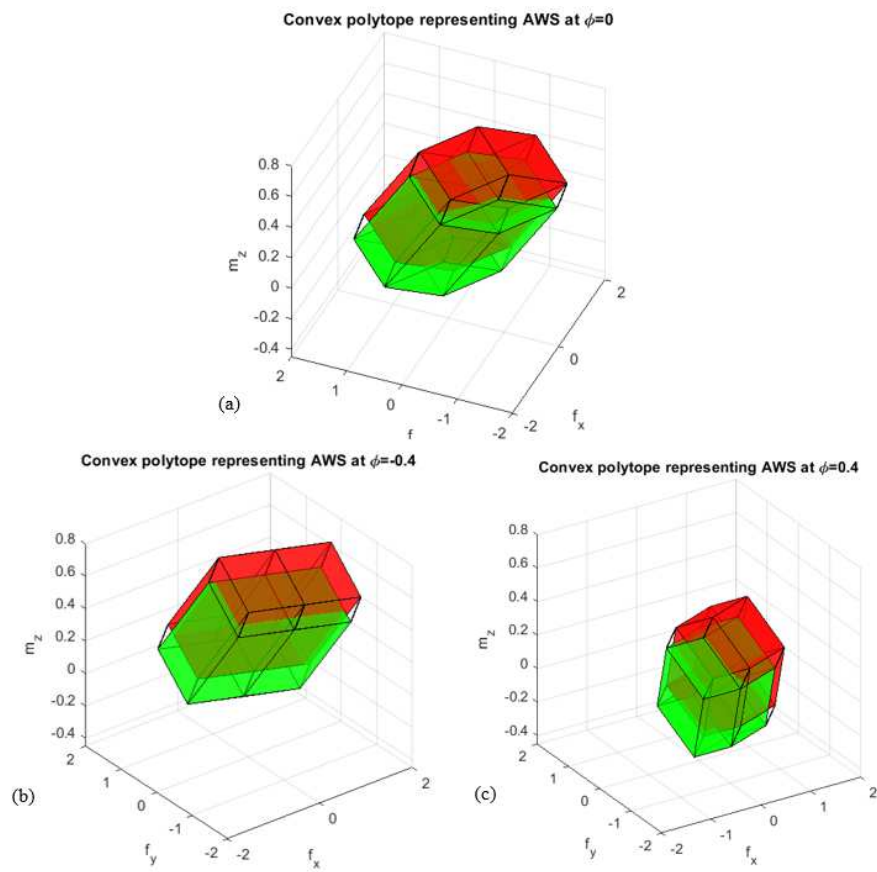


Fig. 4. Convex polytope representing AWS for the 3RPR, 1-PRPR r-CDPR at (a) $\phi_e = 0$ (b) $\phi_e = -0.4$ and (c) $\phi_e = 0.4$

14 A. Raman et al.

$$\phi = \pm 0.4.$$

As the number of actuators in the chain are increased, so do the number of vertices for the wrench polytope. For a 4 cable r-CDPR with 8 actuators, the corresponding wrench polytope contains $2^8 = 256$ vertices. With increasing number of vertices, the creation of polytopes becomes increasingly complex to visualize. Thus for the next case, we will study the wrench polytope of the case with a single mobile base.

4.2 Available Wrench Set for the 3-RPR, 1-PRPR r-CDPR

The wrench polytope for this case is represented in Figure 4. The number of vertices for this structure is 16 (2^5), and similar to the previous figure, red denotes the set of vertex points encapsulating a volume where forces at the slider are maximum and green denotes the set of points encapsulating a volume where forces at the slider are minimum. The individual polytopes themselves are reminiscent of the prior case with 4 cable actuators. The individual hypercubes that comprise this polytope similarly represent the volumes enclosed by cable 1 at its maximum and minimum limit respectively.

In part (b) we notice that as ϕ approaches an extreme limit (-0.4), the forces at the cables reach their limit conditions and can no longer generate a pose with $\phi < -0.4$. Further, the lowest vertex of the polytope lies just above the $m_z = 0$ plane, which indicates that a force with further negative moment can no longer be applied or sustained. However, this is not the case in (c) when ϕ reaches its symmetrically opposite limit of 0.4. These angles are physically realizable due to the additional effect of the mobile slider. The end-effector is capable of sustaining further positive moments at this position indicating that Available Wrench Set at the end-effector is greatly increased simply with the addition of a single mobile base. The true performance and quality of these wrench polytopes over the span of the entire workspace can be evaluated on the basis of better metrics than the pure interpretation of graphical representations and will be part of future work.

5 Conclusion

The wrench formulation through Lie group analysis and subsequent analysis of the wrench polytopes is presented for the fixed fully-constrained planar CDPR and for a reconfigurable CDPR with mobile cable attachment points. Unlike previous established efforts, this approach of formulation does not require the mobile bases and the CDPR to be equilibrated separately. The use of Lie groups was favored here as it aids the formulation (over traditional line-geometry based-screws or vector loop-closure based kinetostatics) because: (a) the modelling lends itself well to generalizations in higher dimensions; and (b) allows direct exploitation of computationally-assisted matrix-vector formulation approaches.

The assembly of the wrench Jacobian is based on the determination of reciprocal wrenches (reciprocal screws) of the individual proper- and redundant- chains. Both parallel mechanisms are redundant, but while a fixed base contains only actuation redundancy, the r-CDPR contains kinematic and further actuation redundancy. The wrench Jacobian can be directly used to graphically represent the true Available Wrench Set at the end-effector that fully represents the tensions at the cable as well as the forces at the mobile bases. We show that with actuation and/or kinematic redundancy at the level of individual chains, the resulting set of wrenches that can be applied and sustained at those poses is significantly increased.

References

1. Agrawal, S.K.: A study of in-parallel manipulators. (1991)
2. Bosscher, P., Ebert-Uphoff, I.: Wrench-based analysis of cable-driven robots. In: IEEE International Conference on Robotics and Automation, 2004. Proceedings. ICRA'04. 2004. vol. 5, pp. 4950–4955. IEEE (2004)
3. Bosscher, P., Riechel, A.T., Ebert-Uphoff, I.: Wrench-feasible workspace generation for cable-driven robots. *IEEE Transactions on Robotics* **22**(5), 890–902 (2006)
4. Bostelman, R.V., Jacoff, A.S., Proctor, F.M., Kramer, T.R., Wavering, A.J.: Cable-based reconfigurable machines for large scale manufacturing (2000)
5. Bouchard, S., Gosselin, C., Moore, B.: On the ability of a cable-driven robot to generate a prescribed set of wrenches (2010)
6. Boudreau, R., Nokleby, S., Gallant, M.: Wrench capabilities of a kinematically redundant planar parallel manipulator. *Robotica* pp. 1–16 (2021)
7. Bruyninckx, H., De Schutter, J.: Unified kinetostatics for serial, parallel and mobile robots. In: *Advances in Robot Kinematics: Analysis and Control*, pp. 343–352. Springer (1998)
8. Erskine, J., Chriette, A., Caro, S.: Wrench analysis of cable-suspended parallel robots actuated by quadrotor unmanned aerial vehicles. *Journal of Mechanisms and Robotics* **11**(2) (2019)
9. Firmani, F., Zibil, A., Nokleby, S.B., Podhorodeski, R.P.: Wrench capabilities of planar parallel manipulators. part i: Wrench polytopes and performance indices. *Robotica* **26**(6), 791 (2008)
10. Firmani, F., Zibil, A., Nokleby, S.B., Podhorodeski, R.P.: Wrench capabilities of planar parallel manipulators. part ii: Redundancy and wrench workspace analysis. *Robotica* **26**(6), 803 (2008)
11. Gagliardini, L., Caro, S., Gouttefarde, M., Girin, A.: Discrete reconfiguration planning for cable-driven parallel robots. *Mechanism and Machine Theory* **100**, 313–337 (2016)
12. Gouttefarde, M., Collard, J.F., Riehl, N., Baradat, C.: Geometry selection of a redundantly actuated cable-suspended parallel robot. *IEEE Transactions on Robotics* **31**(2), 501–510 (2015)
13. Kamali, K., Joubair, A., Bonev, I.A.: Optimizing cable arrangement in cable-driven parallel robots to improve the range of available wrenches (2018)
14. Mohamed, M., Duffy, J.: A direct determination of the instantaneous kinematics of fully parallel robot manipulators (1985)
15. Murray, R.M., Li, Z., Sastry, S.S., Sastry, S.S.: A mathematical introduction to robotic manipulation. CRC press (1994)

16 A. Raman et al.

16. Nguyen, D.Q., Gouttefarde, M.: Study of reconfigurable suspended cable-driven parallel robots for airplane maintenance. In: 2014 IEEE/RSJ International Conference on Intelligent Robots and Systems. pp. 1682–1689. IEEE (2014)
17. Pedemonte, N., Rasheed, T., Marquez-Gamez, D., Long, P., Hocquard, É., Babin, F., Fouché, C., Caverot, G., Girin, A., Caro, S.: Fastkit: A mobile cable-driven parallel robot for logistics. In: Advances in Robotics Research: From Lab to Market, pp. 141–163. Springer (2020)
18. Raman, A., Schmid, M., Krovi, V.: Stiffness modulation for a planar mobile cable-driven parallel manipulators via structural reconfiguration (2020)
19. Rasheed, T., Long, P., Marquez-Gamez, D., Caro, S.: Available wrench set for planar mobile cable-driven parallel robots. In: 2018 IEEE International Conference on Robotics and Automation (ICRA). pp. 962–967. IEEE (2018)
20. Rosati, G., Zanotto, D.: A novel perspective in the design of cable-driven systems. In: ASME International Mechanical Engineering Congress and Exposition. vol. 48739, pp. 617–625 (2008)
21. Weihmann, L., Martins, D., Coelho, L.: Force capabilities of kinematically redundant planar parallel manipulators (2011)
22. Yoshikawa, T.: Manipulability of robotic mechanisms. *The international journal of Robotics Research* 4(2), 3–9 (1985)
23. Zhou, X., Jun, S.k., Krovi, V.: Wrench reconfigurability via attachment point design in mobile cable robots. In: International Design Engineering Technical Conferences and Computers and Information in Engineering Conference. vol. 55935, p. V06AT07A072. American Society of Mechanical Engineers (2013)
24. Zhou, X., Tang, C.P., Krovi, V.: Analysis framework for cooperating mobile cable robots. In: 2012 IEEE International Conference on Robotics and Automation. pp. 3128–3133. IEEE (2012)